Computers and Chemical Engineering 154 (2021) 107500

Contents lists available at ScienceDirect

Computers and Chemical Engineering

journal homepage: www.elsevier.com/locate/compchemeng

A computationally efficient formulation of the governing equations for unit operation design

Andres Carranza-Abaid*, Jana P. Jakobsen

Department of Chemical Engineering, Norwegian University of Science and Technology (NTNU), NO-7491 Trondheim, Norway

ARTICLE INFO

Article history:
Received 9 December 2020
Revised 25 July 2021
Accepted 20 August 2021
Available online 22 August 2021

Keywords:
Modelling
Process design
Numerical analysis
Gas-liquid contactor
CO_2 capture

ABSTRACT

A computationally-efficient numerical method that uses a Pseudo-Eulerian formulation (PEF) for the design calculation of unit operations is presented and validated. This method is applicable to any unit operation that can be modelled using a system of ODEs. Performing the design of a unit operation in the PEF is tenfold faster than with the conventional Eulerian formulation (EF). The mathematical equivalence between the PEF and the EF is demonstrated by proving that the solution of different unit operation design problems provides the same numerical result independently of the formulation. It is shown that reducing the computation of the unit operation design problems also speeds the computation time of a process design or an optimization flowsheet. Additionally, as opposed to other computationally efficient methods for unit operation design, the PEF allows the accurate estimation of the concentration or temperature profiles of complex unit operations such as a multiphase multicomponent reactor system.

1. Introduction

The simulation of chemical engineering processes is a necessary task in the assessment of the techno-economic performance of chemical engineering projects. The flourishment of process simulations can partly be attributed to the steady and constant development of enhanced computer technologies in the recent decades. Although the computational capabilities of modern-day computers have been significantly enhanced over the past years, the computational resources may appear limited with respect to conceptual design and optimization superstructure frameworks. The complexity of these frameworks ultimately may lead to long overall computation times. Undesirable long times are greatly accentuated if the process has unit operations that are designed with ordinary differential equations (ODE). Due to the relevance of ODE-based models for process design, this work will focus on reducing the computation time of ODE systems by proposing a method that derives an alternative formulation of the governing equations.

The unit operation design methods can be divided in two main branches: short-cut methods and rigorous methods. The short-cut methods utilize simplified physics and, hence, do not require complex solution procedures (e.g., the Rayleigh equation in batch distillation, performance equation in reactor design or the height equivalent theoretical plate method for packed columns [HETP]). These methods are usually presented in process design textbooks (e.g. (Levenspiel, 1998; McCabe et al., 2004; Seader and Henley, 2004)) to highlight the fundamental concepts behind the unit operation rather than providing a rigorous description of the physics. On the other hand, rigorous models include different physics phenomena (e.g., thermodynamics and transport phenomena) into the mass and energy conservation equations to account for important effects. It is a common practice to design ODE-based unit operations using the models available in commercial software such as Aspen Plus, CO2SIM or Mathcad. In these cases, a parameter is set (design specification) and an iterative procedure is utilized to find the operating parameter or equipment size that will yield the design specification (e.g., (Cuadri et al., 2020; Lee et al., 2016)). An alternative procedure, applicable for simplified physics, consists in transforming the mathematical model into a set of nonlinear algebraic equations and then using shifted-Legendre polynomials together with the orthogonal collocation method to design the unit operation (Garma et al., 2019).

Despite being computationally efficient, the applicability of the short-cut approaches is limited because they neglect important effects that affect the unit operation design and performance. This causes the short-cut models to have worse prediction capabilities than their rigorous counterparts. For example, by comparing the predictions done by a short-cut model (HETP) (Alhajaj et al., 2016) and a rigorous model (Tobiesen et al., 2007) of an amine-based CO_2 scrubber, it can be observed the later model has superior prediction capabilities of the concentration and temperature profiles.

* Corresponding author.
E-mail address: andres.c.abaid@ntnu.no (A. Carranza-Abaid).

https://doi.org/10.1016/j.compchemeng.2021.107500

Nomenclature

A_C	cross-sectional area [m^2]
a_e	effective specific interfacial area [m^2/m^3]
$\underline{f}$	vector of functions
C	concentration [mol/m^3]
CP	heat capacity [kJ/mol K]
D	diffusivity [m^2/s]
E	energy flow [kJ/s]
H	thermodynamic factor ($H = y/x$) [=]
h_V	heat transfer coefficient [kJ/m^2 s K]
k	mass transfer coefficient [m/s]
K	conductivity [kJ/m K]
L	liquid phase mole flow [mol/s]
P	pressure [kPa]
R	ideal gas constant [kPa m^3/mol K]
T	temperature [K]
V	vapor phase mole flow [mol/s]
v	superficial velocity [m/s]
w	MEA weight fraction in a CO_2-free basis
x	liquid molar fraction
y	vapor molar fraction
Z	compressibility factor [=]
z	height or length of the unit operation [m]
A_C	cross-sectional area [m^2]

Superscript

*	related to the specified variable
r	reduced vector
x	thermodynamic variable *at equilibrium

Subscript

0	bottom of the unit operation
E	related to energy
f	top of the unit operation
i	related to component i
L	related to the liquid phase
spec	the actual value of the specified variable
T	total
V	related to the vapor phase

Greek Letters

α_{CO_2}	CO_2 loading [mol CO_2/mol MEA]
$\underline{\beta}$	state variable vector
ε	absolute error tolerance
θ	independent variable
κ	relative computational speed
λ	heat of phase change [kJ/mol]
μ	viscosity [Pa s]
Ξ	enhancement factor [=]
$\underline{\pi}$	vector of input parameters
ρ	density [kg/m^3]
σ	surface tension [N/m]
φ	fugacity coefficient
χ	reaction constant [1/s]
Ω	relative computational cost

The proper estimation of these profiles is paramount in several unit operations (e.g., heat exchangers or gas-liquid contactors) because their operation and performance can be affected by mass or heat transfer pinch conditions. Considering the need to reduce the computational costs of the simulations without losing the physical meaningfulness of the model, the objectives of this work are:

- Provide a method for developing the governing equations in the Pseudo-Eulerian Formulation (PEF). The PEF extends on the method previously presented in (Carranza-Abaid and Jakobsen, 2020).
- Demonstrate the application of this method to the design of a plug-flow reactor and a gas-liquid contactor for the removal of CO_2.
- Highlight the computational advantages of using the PEF as well as to show that it is possible to reduce the computational costs without oversimplifying the physics.

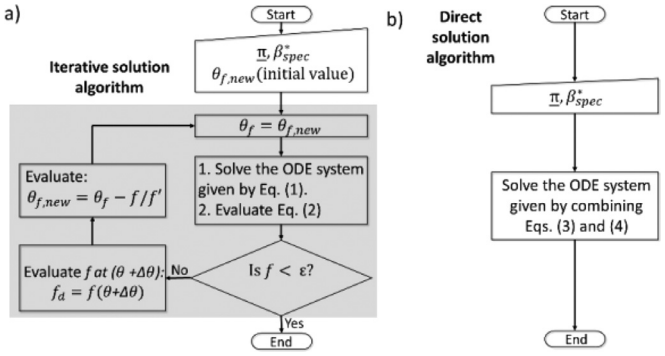

Fig. 1. Algorithm to design a unit operation with a) Eulerian formulation (EF) assuming a Newton-Raphson iterative method and b) Pseudo-Eulerian Formulation (PEF).

2. Methodology

2.1. Eulerian formulation

The differential equations describing the property flows (mass and energy flows) can be derived using the Eulerian formulation (EF) or the Lagrangian formulation (LF). The difference between both formulations is the frame of reference used to derive the equations and the chosen control volume. The EF uses a control volume that is fixed in space; thus, it quantifies the property flow field from a stationary location. On the other hand, the control volume in the LF moves with the flow field, hence it quantifies the property flow field using a moving location. Of the two, the EF is more used, perhaps because of its computational advantages (Jakobsen, 2014) or its simpler way of formulating and solving the governing equations.

The main characteristic of the EF is that the property flows are the state variables, and the spatial dimension of the system is the independent variable. The general form of a 1-D model can be expressed as a vector of state variables ($\underline{\beta}$) that are a function of an independent variable (θ) and a set of parameters ($\underline{\pi}$):

$$\frac{d}{d\theta}\left(\underline{\beta}(\theta)\right) = \underline{f}\left(\underline{\beta}(\theta), \underline{\pi}\right) \tag{1}$$

Note that the independent variable can be either a spatial or temporal dimension. The simulation of a unit operation described by Eq. (1) usually means solving a boundary value problem (BVP) where the boundary conditions of each one of the dependent variables must be specified in addition to the boundary where those conditions apply (θ_0 or θ_f).

Unit operation design calculation implies that the value of a state variable at a given location in the unit operation is specified (usually it is when $\theta = \theta_f$). The unit operation design specification fixes the state variable (β^*_{spec}) at a certain θ_f. Since the value of θ_f is an unknown variable of the design problem and, at the same time, it is needed to solve Eq. (1), an iterative procedure is needed (see Fig. 1a). A discrepancy function is then applied to evaluate how far the calculated specified state variable (β^*) is from the specified value (β^*_{spec}). For a constant set of input parameters $\underline{\pi}$, the evaluation of the discrepancy function (f) must be equal or

below a specified tolerance (ε):

$$f = \left|\beta^*(\theta) - \beta^*_{spec}(\theta)\right| \leq \varepsilon \tag{2}$$

Fig. 1a illustrates that it is computationally expensive to solve a BVP problem in order to comply with Eq. (2) because of the iterative nature of the algorithm which is causing a computational bottle neck in the unit operation design calculation.

It is important to remark that a unit operation can be designed if and only if the solution of the state variables satisfies $\underline{\beta} \in \mathbf{R}$. Unit operation design calculation implicitly assumes that the solution is within physical boundaries, hence if there is no solution, the algorithm will not converge (the program may even crash in some cases if complex numbers appear during the calculations).

2.2. Pseudo-Eulerian formulation

This formulation is based on deriving the governing equations as a function of β^* instead of θ. The way to do this is to apply the chain rule between the vector of derivatives and the inverse of the ODE that describes the specified state variable. In this way, the new ODE system expresses the state variables (the ones that are not the specified state variable $\underline{\beta}^r$) as a function of the specified state variable. This procedure gives the following governing equations with the PEF:

$$\frac{d}{d\beta^*}\left(\underline{\beta}^r(\beta^*)\right) = \underline{f}^r\left(\underline{\beta}^r(\beta^*), \underline{\mu}\right) \tag{3}$$

Note that $\underline{\beta}^r$ is a reduced vector with *c-1* variables. The PEF ODE system has a reduced geometry when compared to the ODE of the EF. This is because the procedure to derive the PEF equations makes the equation corresponding to the specified variable a trivial solution. The form of Eq. (3) implies that when the system can be conceived within the physical boundaries ($\underline{\beta} \in \mathbf{R}$), all the mass and energy balances are relative to each other, hence, one can calculate how the state variables behave as a function of the specified state variable.

As seen in Fig. 1b, solving the ODE set given by Eq. (3) provides the solution of the mass and energy balances, but it does not calculate the final design of the unit operation. This is because the ODE set is relative to $\beta^*$and the solution is then in a "dimensionless" mathematical space that is not dependent on the spatial or temporal dimensions. Because of its mathematical properties and the physical implications of the PEF of the governing equations, it can be considered that the mass and energy balances are formulated in a different frame of reference than in the EF.

It should be noted that if the problem does not require to design the unit operation (i.e., the equipment volume is not needed), then it is enough to solve the equations with the form of Eq. (3). This can save further computation time since the extra computational resources needed to give the system spatial dimensions are avoided.

On the other hand, if the unit operation design is needed, one must bring the solution from the dimensionless mathematical space to the spatial or temporal dimensions. This is done by adding a “dimensioning” function to the ODE system. This equation has the general form:

$$\frac{d\theta}{d\beta^*} = f^*\left(\underline{\beta}^r(\beta^*), \underline{\mu}\right) \tag{4}$$

Note that the ODE of Eq. (4) is the reciprocal of the ODE that describes the state variable behavior in the EF.

3. Results

This section presents the application of the PEF for two different unit operation design problems. The first example highlights the numerical and conceptual equivalence between the EF and the PEF models and shows the computational gains of using the PEF. The second example validates PEF-based model of a multiphase multicomponent reactor and discusses the effect of the computational advantages of using the proposed method on a superstructure framework.

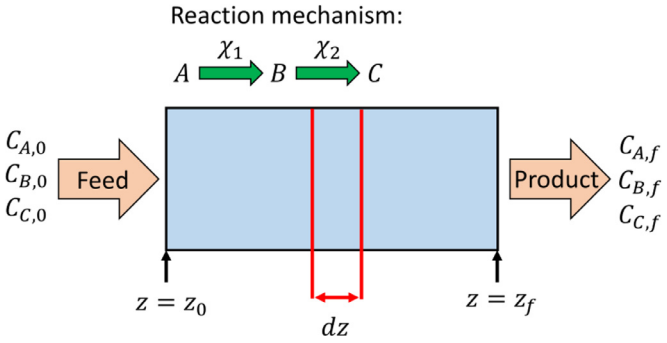

Fig. 2. Sketch of the modelled tubular reactor with two reactions in series.

3.1. Multiple reactions in an ideal plug-flow reactor

This subsection presents the implementation of the PEF for the design of an ideal plug-flow reactor (Fig. 2). The reaction mechanism is illustrated in Fig. 2 and each one of the reactions has a first order kinetic behavior. The model considers a reactive liquid phase system with constant density that operates under an isothermal plug-flow hydrodynamic regime where the diffusivity of the components is infinitely slow compared to the reaction rate.

Eulerian Formulation: The equations and the boundary conditions that model the plug-flow reactor are:

$$\frac{dC_A}{dz} = -\frac{\chi_1 C_A}{v} \qquad B.C.: \; C_A = C_{A,0} \; for \; z = z_0 \tag{5}$$

$$\frac{dC_B}{dz} = \frac{\chi_1 C_A}{v} - \frac{\chi_2 C_B}{v} \qquad B.C.: \; C_B = C_{B,0} \; for \; z = z_0 \tag{6}$$

$$\frac{dC_C}{dz} = \frac{\chi_2 C_B}{v} \qquad B.C.: \; C_C = C_{C,0} \; for \; z = z_0 \tag{7}$$

The design problem consists in finding the reactor volume that yields a certain amount of component A, therefore, the discrepancy function is:

$$f = \left|C_{A,f} - C_{A,f|spec}\right| \leq \varepsilon \tag{8}$$

Pseudo-Eulerian formulation: considering the same assumptions and using the concentration of component A as the independent variable, the equations are:

$$\frac{dC_B}{dC_A} = -\frac{\chi_1 C_A - \chi_2 C_B}{\chi_1 C_A} \qquad B.C.: \; C_B = C_{B,0} \; for \; C_A = C_{A,0} \tag{9}$$

$$\frac{dC_C}{dC_A} = -\frac{\chi_2 C_B}{\chi_1 C_A} \qquad B.C.: \; C_C = C_{C,0} \; for \; C_A = C_{A,0} \tag{10}$$

$$\frac{dz}{dC_A} = -\frac{v}{\chi_1 C_A} \qquad B.C.: \; z = z_0 \; for \; C_A = C_{A,0} \tag{11}$$

The key difference between the EF and the PEF is that while the PEF express the concentration values of components B and C when the concentration A has certain value ($C_{A,0}$), the B.C. in the EF express the concentration values of A, B, C where the inlet is being fed. From a practical point of view, both formulations “answer” different questions. While the EF answers: “what happens to the component concentrations in a reactor with certain spatial dimensions?”, the PEF answers: “what should happen in the reactor to achieve this concentration of this component?”.

The PEF can also be utilized in the design of processes where time is the independent variable (batch or semi batch processes

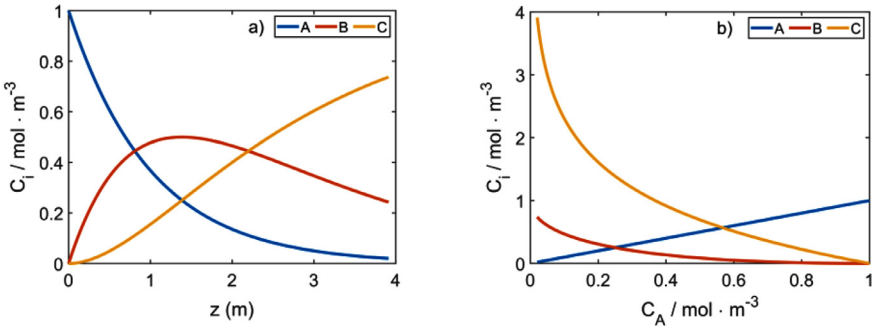

Fig. 3. Concentration profiles obtained with solution of the ODE set given by the a) Eulerian formulation (EF) and b) Pseudo-Eulerian formulation (PEF). Parameters ($\underline{\pi}$): $C_{A,0} = 1\ mol\ m^{-3}$, $C_{B,0} = C_{C,0} = 0\ \ mol \cdot m^{-3}$, $\chi_1 = 1\ s^{-1}$, $\chi_2 = 0.5\ s^{-1}$ and $\nu = 1.0\ m \cdot s^{-1}$. Design spec: $C_{A,f} = 0.02\ \ mol \cdot m^{-3}$.

like reactors or drying systems). If we apply the reaction scheme shown in Fig. 2 to a batch reactor, Eqs. (9-11) will have a similar form with minor differences: the independent variable would be time (t) instead of length (z) and Eq. (11) will not have the surface velocity term (ν). The resulting set of ODEs would find the time t needed to reach certain concentration. It should be noted that in this case, the design of the unit operation does not include the estimation of the physical dimensions of the reactor, which can be easily estimated with an algebraic equation that involves time and the initial amount of reactants as it has traditionally been done in reactor design (Levenspiel, 1998).

Transforming an already-implemented EF model into a PEF is a straightforward task that requires few modifications in the EF programming code. It is enough to evaluate the equations in their EF (form of Eq. (1)) and then multiply the numerical result by the inverse of the ODE containing the design specification. Note that the ODE containing the design specification must be multiplied twice in order to obtain the inverse of the design specification derivative (Eq. (11) was estimated by multiplying Eq. (5) by its inverse two times). Moreover, the boundary conditions should also be modified according to the change of independent variables, however, as seen in Eqs. (9-11), the numerical values are the same as in the EF.

In order to illustrate the equivalence between both formulations, a design calculation was performed of a plug-flow reactor that converts 98 % of an inlet stream that only contains 1 $mol\ m^{-3}$ of component A (see Fig. 2). Fig. 3 presents the obtained concentration profiles of the 3 components as a function of the independent variable. Fig. 3a is done by solving Eqs. (5-8) with the algorithm presented in Fig. 1a while Fig. 3b is the solution of Eqs. (9-11). The "spaceless" concentration profiles of Fig. 3b can be transformed into the spatial-dependent concentrations profiles shown in Fig. 3a by evaluating Eq. (11).

Both ODE systems are solved with the orthogonal collocation fifth-order method available in Matlab 2019b (bvp5c function). For the case of the EF, the Newton-Raphson numerical method was used to find the solution to the design problem by solving the discrepancy function.

The equivalence between the EF and the PEF can be assessed by calculating the average absolute relative deviation (AARD) between the numerical results of both formulations. The AARD was calculated using the following equation:

$$AARD = \frac{1}{N}\sum_{1}^{N}\left|\frac{(Y_{EF} - Y_{PEF})}{\sqrt{(Y_{EF})(Y_{PEF})}}\right| \tag{12}$$

Where N is the total number of compared simulations, Y_{EF} and Y_{PEF} are the output variables calculated using the EF and PEF respectively.

An analysis of the computational speed and the numerical equivalence between both formulations was done by performing the simulations for the presented problem at different operating conditions. The Monte Carlo method was used to randomly generate the input parameters of 1,000 design problems from which the computational speed and the numerical difference between selected output variables ($C_{A,f}, C_{B,f}$, $C_{C,f}$ and z_f) was assessed. The varied input parameters and their respective ranges are shown in Table 1 and the remaining parameters have the same values as used in the calculations needed in Fig. 3. The initial value to start the iterations in the EF calculations to obtain the required z_f was set to be equal to 1 m.

Table 1
Limits of the varied parameters in the Monte Carlo simulations.

Parameter	Min	Max
χ_1 / $mol \cdot m^{-3} \cdot s^{-1}$	0.5	3.0
χ_2 / $mol \cdot m^{-3} \cdot s^{-1}$	0.01	0.5
ν / $m \cdot s^{-1}$	0.5	1.5
$C_{A,F}$ / $mol \cdot m^{-3}$	0.01	0.99

Although both models use the same BVP solver, it is important to remark that the PEF does not require a discrepancy function to solve the design problem specifications, therefore, the entire computation time is spent on solving a single BVP problem. Contrarily, the EF requires to specify the tolerance of the discrepancy function (ε), which impacts the computational cost of the design problem as seen in Fig. 4. The computational cost is defined as the number of times the ODE system is evaluated to solve a single design problem (i.e., the number of times the Matlab function containing the ODE system is evaluated). The relative computational cost (Ω) is defined as

$$\Omega = \frac{EF\ computational\ cost}{PEF\ computational\ cost} \tag{13}$$

Fig. 4 presents two probability histograms as a function of Ω. The histograms use the same sampling sets but different discrepancy function tolerances. The tolerance in Fig. 4a is set to be $\varepsilon = 10^{-5}$ while for Fig. 4b $\varepsilon = 10^{-9}$. In both cases the probability of decreasing the computational costs by more than 5 times is $>$ 95 % while for an entire order of magnitude is over 60 % for Fig. 4a and 75 % for Fig. 4b. If one compares Fig. 4a and Fig. 4b, it is possible to notice that the lower the tolerance, the larger the computational speed-up. This situation occurs because lower tolerances require more iterations in the Newton Raphson while the computational cost for the PEF remains constant because the design specification is fed as the upper boundary of the independent variable ($C_{A,f}$). This proves that the removal of the iteration loop in the algorithm (Fig. 1) makes the operation unit design calculation more efficient.

One may wonder, how does the computational cost relate with the computational speed and does it speed-up the calculations? To

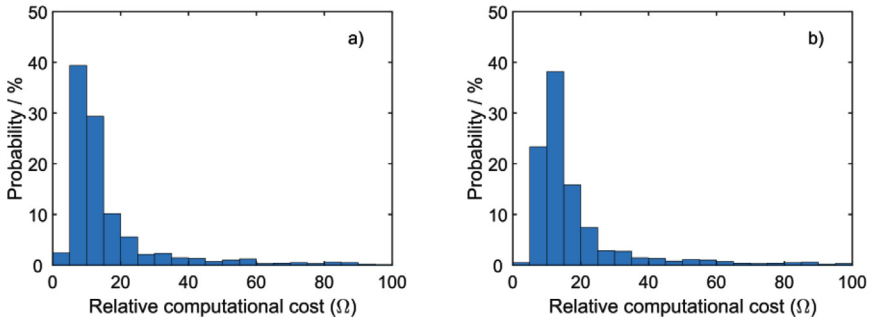

Fig. 4. Probability distribution of the relative computational cost (ε) at different discrepancy function tolerance: a) $\varepsilon = 10^{-5}$ and b) $\varepsilon = 10^{-9}$.

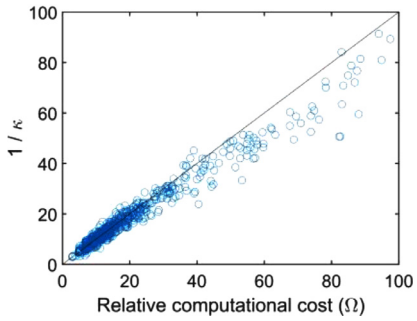

Fig. 5. The reciprocal of the relative computational speed versus the relative computational costs between the Eulerian and the pseudo-Eulerian formulations.

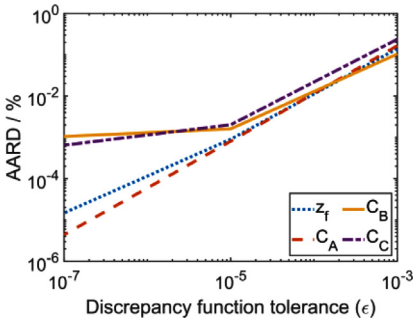

Fig. 6. The AARD between the numerical solutions of the EF and the PEF equations for the ideal plug-flow reactor study.

answer this question, a parity plot between Ω and the inverse of the relative computational speed ($1/\kappa$) is shown in Fig. 5. The relative computational speed is calculated with the following equation:

$$\kappa = \frac{EF\ computational\ speed}{PEF\ computational\ speed} \tag{14}$$

Fig. 5 shows that the relative computational cost is inversely proportional to the relative computational speed. Therefore, reporting Ω or $1/\kappa$ is approximately equivalent. It is important to remark that, although reporting the relative computational time may give a more meaningful insight to the end-user, computation times are subject to the available computing resources and other variables that are outside the scope of this discussion. For this reason, it is more convenient to compare the computational costs of algorithms instead of the computation time.

Both formulations are equivalent from a mathematical standpoint. However, the comparison of obtained solutions may exhibit discrepancies caused by the non-exact nature of the numerical method used to solve the ODEs and the fact that the EF uses a discrepancy function, hence the calculated $C_{A,f}$ will be different from $C_{A,f|spec}$. In contrast, the PEF uses $C_{A,0}$ and $C_{A,f}$ as the limits of the independent variable, therefore, $C_{A,f} = C_{A,f|spec}$. The difference between solutions obtained from both formulations was assessed and it is presented in Fig. 6. It shows that the AARD substantially decreases when the discrepancy function of the EF is $\varepsilon \geq 10^{-7}$ for all the output variables.

3.2. Multicomponent multiphase reactor

3.2.1. PEF governing equations

This subsection presents the validation of a multicomponent multiphase reactor PEF-based model. The studied case is the CO_2 capture from a flue gas using an amine-based absorption relevant to both the chemical and the environmental engineering field. Absorbers for CO_2 capture are usually designed to remove a specified amount of CO_2 from a given flue gas, hence, developing the governing equations in the PEF can be particularly advantageous.

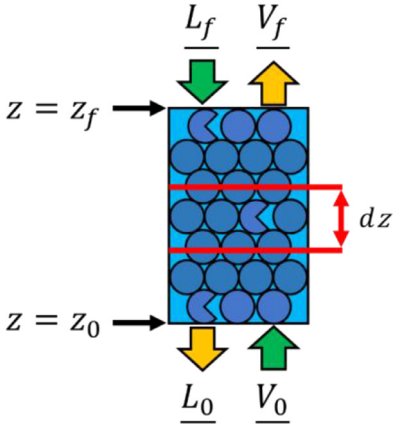

Fig. 7. Sketch of the modelled multicomponent multiphase reactor. $\underline{V}$ and $\underline{L}$ represent the property flows of the vapor and liquid phases respectively.

A sketch of the modelled system is presented in Fig. 7. The following considerations were done in the model development:

1. The process is adiabatic, isobaric and is operated in steady state.
2. The vapor and liquid phases have a plug-flow hydrodynamic regime.
3. There are four components in the system: CO_2, monoethanolamine (MEA), H_2O and N_2.
4. N_2 is not soluble in the liquid phase.
5. The direction of the mass and energy transfer is assumed to be from the vapor phase to the liquid phase.
6. All thermal effects related to phase-shifting take place in the liquid phase.
7. The energy transport in the liquid phase is infinitely fast compared to the vapor phase.

Table 2
Description of the parameters used in the model validation of the gas-liquid contactor.

System	Parameter	Comment	Reference
1,2	Z	Peng - Robinson	(Peng, 1976)
1,2	φ_i	Peng - Robinson	(Peng, 1976)
1,2	$H_i,\ P^*,\ P_i^*$	Machine learning based surrogate thermodynamic model	(Carranza-Abaid et al., 2020)
1	$a_e, k_{V,i},\ k_{L,i}$	Random packing (Berl saddles)	(Bravo and Fair, 1982; Onda et al., 1968)
2	$a_e, k_{V,i},\ k_{L,i}$	Structured packing (Mellapak 250Y)	(Rocha et al., 1993; Suess and Spiegel, 1992)
1,2	E	Irreversible enhancement factor	(Luo et al., 2015)
1,2	h_V	Chilton-Colburn analogy	(Chilton and Colburn, 1934)

According to assumptions #1 to #3, the model is independent of time and the state variables only vary along the axial dimension. Following the nomenclature of Fig. 7, the resulting equations in the PEF are:

$$\frac{dV_i^r}{dV_{CO_2}} = \frac{r_i^r}{r_{V,CO_2}} \ (i \neq CO_2) \qquad B.C.:\ V_i^r = V_{i,0}^r \ for\ V_{CO_2} = V_{CO_2,0} \tag{15}$$

$$\frac{dL_i}{dV_{CO_2}} = \frac{r_i}{r_{V,CO_2}} \qquad B.C.:\ L_i = L_{i,f} \ for\ V_{CO_2} = V_{CO_2,f} \tag{16}$$

$$\frac{dE_V}{dV_{CO_2}} = \frac{r_{E,V}}{r_{V,CO_2}} \qquad B.C.:\ E_V = E_{V,0} \ for\ V_{CO_2} = V_{CO_2,0} \tag{17}$$

$$\frac{dE_L}{dV_{CO_2}} = \frac{r_{E,L}}{r_{V,CO_2}} \qquad B.C.:\ E_L = E_{L,1} \ for\ V_{CO_2} = V_{CO_2,f} \tag{18}$$

$$\frac{dz}{dV_{CO_2}} = -\frac{1}{A_C r_{V,CO_2}} \qquad B.C.:\ z = z_0 \ for\ V_{CO_2} = V_{CO_2,0} \tag{19}$$

The form of the mass energy balance equations for gas-liquid contactors in the EF can be consulted in the literature (Faramarzi et al., 2010; Gabrielsen et al., 2007; Taylor and Krishna, 1993; Tobiesen et al., 2007; Tontiwachwuthikul et al., 1992).

The system of ODEs contains 8 equations from which 2 ODEs with the form of Eq. (15), 3 ODEs with the form of Eq. (16) and one ODE for each one of the remaining equations. Because of assumption #4, the evaluation of the ODEs corresponding to N_2 are always 0 and therefore can be eliminated from the ODE set. Furthermore, it is important to remark that although there are electrolyte compounds in the liquid mixture (caused by the solubilization of CO_2), their mass balances are lumped into the apparent mass balances of CO_2, MEA and H_2O.

The source terms in the above equations are estimated using an overall mass or energy transfer coefficient. Considering assumption #5, the rate term for component i can be defined by:

$$r_i = \left[\frac{1}{\frac{ZRT_V}{a_e k_{V,i}} + \frac{H_i \varphi_i P^x}{\Xi a_e k_{L,i} C_L}}\right]\left(P_i - P_i^x\right) \tag{20}$$

Note that the overall mass transfer coefficient is the term inside the square brackets. The first term in the denominator is the resistance to the mass transfer in the vapor phase while the second term corresponds to the liquid phase resistance. The enhancement factor term (Ξ) only applies to the CO_2 rate of mass transfer.

Since assumption #6 implies that the liquid phase gives or removes the necessary amount of energy from the molecule that is going to be transferred between both phases the energy source terms are:

$$r_{E,V} = \left[\frac{1}{\frac{1}{a_e h_V}}\right](T_V - T_L) + \sum_i^n r_i H_{V,i} \tag{21}$$

$$r_{E,L} = \left[\frac{1}{\frac{1}{a_e h_V}}\right](T_V - T_L) + \sum_i^n r_i (H_{V,i} - \lambda_i) \tag{22}$$

Assumption #7 implies that the overall energy transfer coefficient is only a function of the vapor phase resistance to energy transfer. The enthalpy of phase change (λ_i) is estimated using a rigorous method that sums the enthalpies of vaporization and reaction (Kim et al., 2009).

3.2.2. Complementary Equations and Parameters

The model validation was performed by comparing the simulated results with the measured values from different pilot plant systems reported in the open literature. A summary of the equations used to describe the absorber transport phenomena and thermodynamics is presented in Table 2.

Two different systems are used as the benchmark to validate the absorber model. System 1 refers to the data measured in a random packed column (Tontiwachwuthikul et al., 1992) and system 2 refers to the experimental data obtained in a structured packed column (Tobiesen et al., 2007). Since the packing material in the experimental setups is different, the correlations to describe the mass transfer coefficients will differ as well.

The correlations used in the gas-liquid contactor model require certain properties of the gas and liquid phases to be estimated. The methods used to estimate the physical properties are shown in Table 3. The properties labeled as machine learning models in Table 3 use a shallow neural network architecture. The models, their parameters and their statistical analysis are presented in the supporting information.

3.2.3. Model application

This subsection shows that, as opposed to shortcut methods, the PEF allows the proper estimation of the profiles of the process parameters. As discussed in Section 1, it is important for the unit operation models to properly estimate the location of the mass and energy transfer pinch points because they affect the absorber performance (Kvamsdal and Rochelle, 2008). As it can be seen in the profiles of α_{CO_2}, y_{CO_2}, T_V and T_L in Fig. 8, the calculations not only have good agreement with the stream outlet values, but also on the mass and energy balances profiles. Fig. 8 shows a proper prediction of the temperature bulges that are commonly observed in CO_2-amine systems. In the cases of Fig. 8 a) – c), the bulge is located at the bottom of the absorber whereas in Fig. 8 d) is located close to the top of the absorber. This is because the relation between the liquid and vapor flows (L/V ratio) in system 1 is larger than in system 2, which means that lower L/V ratios move the bulge location higher in the column. The validation of other important process variables is presented in the supporting information S2.

In the same fashion as in the previous example, a Monte Carlo method was used to perform 1,000 simulations in order to assess the difference between using the EF or the PEF. The simulations were done using the packing specifications of system 2 and varying the inputs inside the ranges shown in Table 4 considering a tolerance for the discrepancy function of $\varepsilon = 10^{-7}$. The results of the Monte Carlo simulations are presented in Table 5. The difference between the solutions of both models is negligible for practical purposes as the AARD between all the important variables is

Table 3
Methods to estimate the properties of the gas-liquid contactor.

Property	Comment	Reference
ρ_V	Peng-Robinson	(Peng, 1976)
K_V	Non-linear mixing rule and correction for higher pressures	(Misic and Thodos, 1961; Stiel and Thodos, 1964; Wassiljewa, 1904)
μ_V	Non-linear mixing rule and correction for higher pressures	(Bromley and Wilke, 1951; Misic and Thodos, 1961; Stiel and Thodos, 1964)
$D_{i,V}$	Predictive method of the binary diffusion coefficients	(Fuller et al., 1966)
CP_V	DIPPR equation	Parameters taken from Aspen Plus v8.6 Databank
ρ_L	In-house machine learning model	(Amundsen et al., 2009; Hartono et al., 2014; Weiland et al., 1998)
σ_L	In-house machine learning model	(Amundsen et al., 2009; Hartono et al., 2014; Korson et al., 1969; Weiland et al., 1998)
μ_L	In-house machine learning model	(Idris et al., 2017; Jayarathna et al., 2013a, 2013b; Vázquez et al., 1997)
$D_{i,L}$	Empirical correlation for alkanolamine solutions*	(Snijder et al., 1993)

* $D_{H_2O,L}$ is held constant and equal to 10^{-9} m^2/s

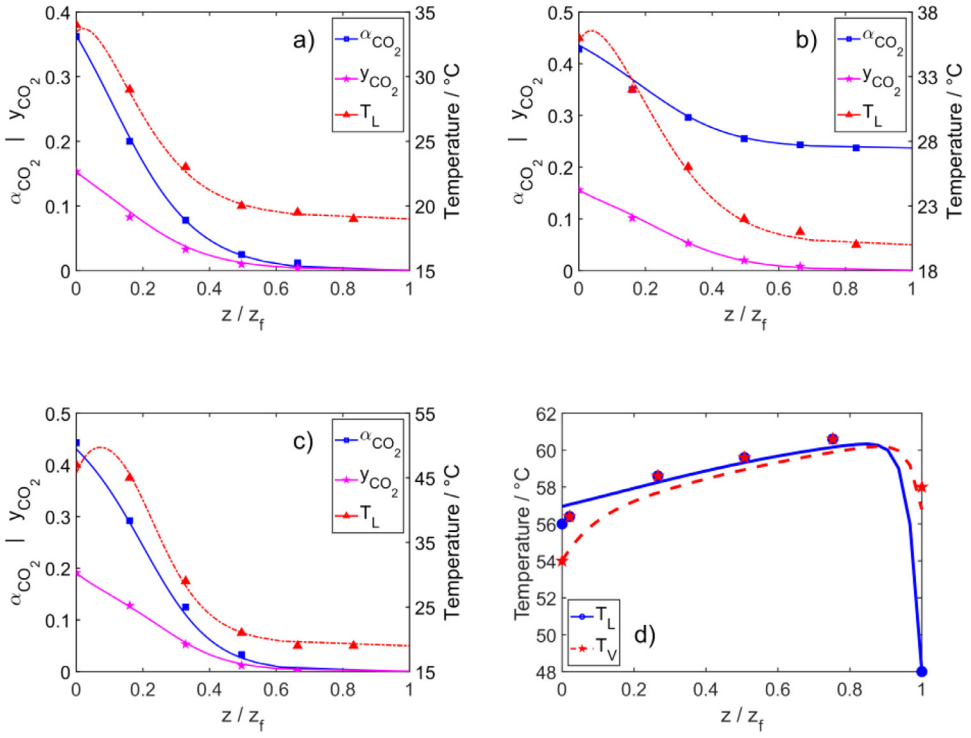

Fig. 8. Comparison between the model predictions and the corresponding experimental values at different operating conditions: a) run 13 (system 1), b) run 17 (system 1), c) run 22 (system 1) and d) run 10 (system 2).

Table 4
Limits for the Monte Carlo simulations in the absorber case study.

Variable	Min.	Max.
$y_{CO_2,0}$	0.003	0.10
$y_{CO_2,0}$	0.01	0.2
$\alpha_{CO_2,0}$	0.1	0.25
L / V	6	12
T_L, T_V / °C	40	
$V_{0,T}$ / mol/s	1	
w_{MEA} / %	30	

Table 5
Difference between the EF and PEF of selected output variables of the absorber model.

Variable	AARD / %	Max. AARD / %
z_f	8×10^{-7}	1×10^{-5}
$y_{CO_2,1}$	5×10^{-5}	2×10^{-4}
$\alpha_{CO_2,0}$	5×10^{-9}	1×10^{-8}
$T_{V,1}$	2×10^{-6}	8×10^{-5}
$T_{L,0}$	9×10^{-7}	2×10^{-5}

less than 10^{-6} which means that the relative deviation is caused by the inherent error of the BVP solver used and the iterative loop needed to obtain the dimensions of the absorber in EF.

The comparison of the computational costs between both formulations is given in Fig. 9. This histogram has a similar shape as in the first plug-flow example (Fig. 4). It shows that for a gas-liquid contactor, a speed-up of around one order of magnitude is expected. Although the computational costs may differ from system to system, the relative computational costs of the PEF seem to be, in average, around one order of magnitude.

Another advantage of the PEF over the EF is when an unfeasible design is proposed as a specification (i.e., when the solution of the state variables $\underline{\beta} \notin \mathbf{R}$). It was noticed that when the EF is used to solve the problem, the procedures run for a long time because the iterative algorithm diverges until either the program "crashes" or the maximum number of iterations is reached. Whereas the PEF quickly finds which solution is not feasible and hence stops the calculations earlier without spending additional computational resources.

From the end-user point of view, spending 1.5 seconds instead of 0.1 seconds to design a single unit operation is more a minor inconvenience rather than a fatal issue. However, unit operations are

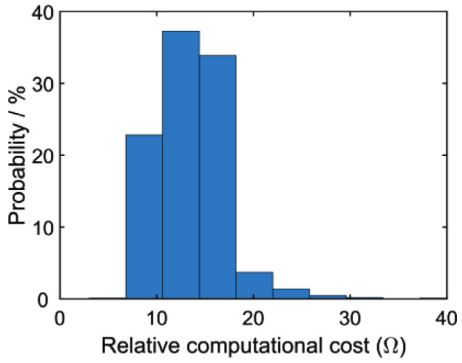

Fig. 9. Results of the relative computational cost between the EF over the PEF.

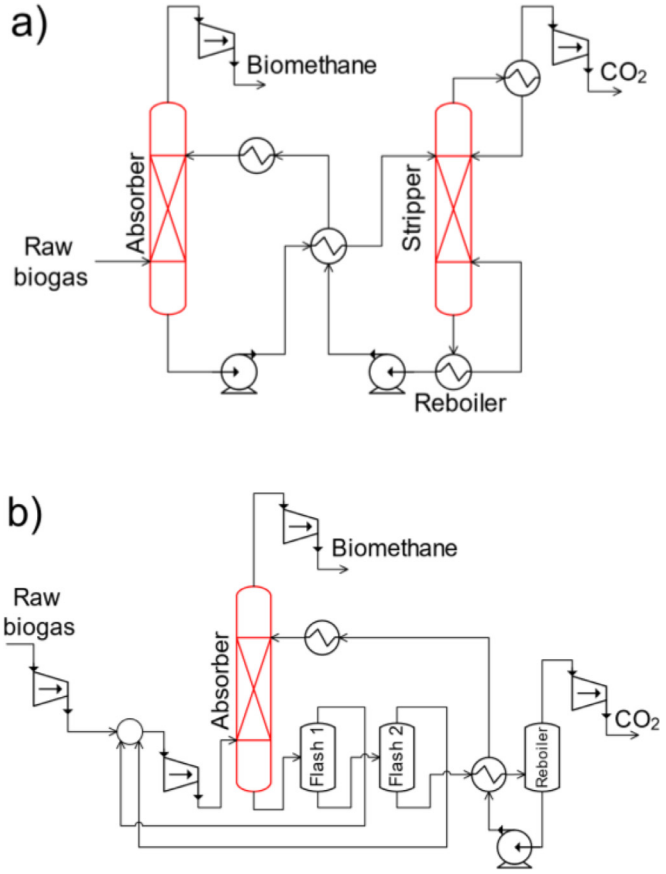

Fig. 10. Biogas upgrading technologies a) Aqueous amine process b) Physical-solvent process.

usually part of larger processes and optimization superstructure frameworks. Using the PEF in the evaluation of these frameworks is beneficial because if the unit operation speed can be reduced more than ten times, their overall computation speed should also be reduced accordingly.

To illustrate this, let us take the examples of the biogas upgrading processes shown in Fig. 10 that remove the CO_2 from the raw biogas to produce biomethane (Carranza-Abaid et al., 2021). Fig. 10a shows the amine-based biogas upgrading process, which contains two unit operations that are designed with ODE-based models (marked in red). In order to test the PEF computational advantages, this process was designed and optimized by manipulating the solvent flowrate, amine concentration and desorber pressure. It was found that utilizing the PEF for optimization frameworks can be 9-20 times faster than with the EF. These values agree with those shown in Fig. 9 because more than 99 % of the computational time is spent on the design of the absorber and the stripper. Conversely, designing the physical solvent process (Fig. 10b) with the PEF, a computational speed is around 7 to 16 times faster. Although still quite high, the computational advantages of the PEF are not as high as in the amine process because in the second process. In this case only 80 % of the computational time is spent on the absorber because the calculations involved in the flash tanks, recirculation compressors and reboiler are computationally intensive as well. The same relative computational speed up is observed when any of the two processes is designed at fixed conditions or when the processes are optimized.

Reducing the computation time of any process superstructure framework has great practical potential since it is quite convenient for the analysis and selection of materials such as chemical solvents for CO_2 removal. If one wants to assess the techno-economic potential of a novel solvent for CO_2 capture, it necessary to have a mixed-integer optimization framework that considers multiple process parameters, several process configurations, and other relevant variables (e.g., plant location or solvent supplier). Instead of unnecessarily spending days or even weeks in evaluating all the possible scenarios for an optimization, one could perform the same comprehensive analysis in few hours by reformulating the models with the PEF. This approach is not only limited for solvent-based technologies since the PEF can be utilized in other superstructure frameworks that involve other processes such as simple distillation (packed column), reactive distillation, membrane separation, adsorption or batch processes.

4. Conclusions

A Pseudo-Eulerian formulation (PEF) was proposed to develop the governing equations for the design calculation of unit operations. It was shown that this alternative formulation (PEF) speeds-up the unit operation design algorithm by removing the inherent iterative loop that arises from developing and solving the governing equations in the Eulerian framework. It was demonstrated that utilizing the PEF algorithm for unit operation design is more than tenfold faster than the EF algorithm. The solution of the PEF-based model gives similar numerical results as the EF-based models with minimal numerical differences that can be attributed to the numerical methods.

The PEF approach was used, as an example, to model a multiphase multicomponent reactive system (CO_2 absorber). It was shown that, as opposed, to the short-cut methods, it can properly represent the mass and temperature profiles. This shows that there is no need to oversimplify the physics of the unit operations to implement computationally fast unit operation design algorithms.

Using the PEF to develop unit operation design models can be utilized for greatly improving the computational speed of rigorous superstructure frameworks that involve conceptual process design such as the ones utilized in sensitivity, optimization, or uncertainty quantification studies. The computational advantages of the PEF are more significant when there is a larger number of unit operations that are modelled with an ODE.

Declaration of Competing Interest

The authors do not declare conflict of interest in this article.

CRediT authorship contribution statement

Andres Carranza-Abaid: Conceptualization, Methodology, Software, Validation, Formal analysis, Investigation, Data curation, Writing – original draft, Writing – review & editing, Visualization.

Jana P. Jakobsen: Conceptualization, Resources, Supervision, Writing – review & editing, Project administration, Funding acquisition.

Acknowledgments

This research was funded by the Faculty of Natural Sciences of the Norwegian University of Science and Technology (NTNU).

Supplementary materials

Supplementary material associated with this article can be found, in the online version, at doi:10.1016/j.compchemeng.2021.107500.

References

Alhajaj, A., Mac Dowell, N., Shah, N., 2016. A techno-economic analysis of post-combustion CO2 capture and compression applied to a combined cycle gas turbine: Part I. A parametric study of the key technical performance indicators. Int. J. Greenh. Gas Control 44, 26–41. doi:10.1016/j.ijggc.2015.10.022.

Amundsen, T.G., Oi, L.E., Eimer, D.A., 2009. Density and viscosity of monoethanolamine plus water plus carbon dioxide from (25 to 80) degrees C. J. Chem. Eng. Data 54 (11), 3096–3100. doi:10.1021/je900188m, https://doi.org/10.1021. J. Chem. Eng. Data 54, 3096-3100Amundsen, T. G., Oi, L. E., Eimer, D. A..

Bravo, J.L., Fair, J.R., 1982. Generalized correlation for mass transfer in packed distillation columns. Ind. Eng. Chem. Process Des. Dev. 21, 162–170. doi:10.1021/i200016a028.

Bromley, L.A., Wilke, C.R., 1951. Viscosity behavior of gases. Ind. Eng. Chem. 43, 1641–1648. doi:10.1021/ie50499a046.

Carranza-Abaid, A., Jakobsen, J.P., 2020. A non-autonomous relativistic frame of reference for unit operation design. In: Computer Aided Chemical Engineering, pp. 151–156. doi:10.1016/B978-0-12-823377-1.50026-4.

Carranza-Abaid, A., Svendsen, H.F., Jakobsen, J.P., 2020. Surrogate modelling of VLE: integrating machine learning with thermodynamic constraints. Chem. Eng. Sci. X 8, 100080. doi:10.1016/j.cesx.2020.100080.

Carranza-Abaid, A., Wanderley, R.R., Knuutila, H.K., Jakobsen, J.P., 2021. Analysis and selection of optimal solvent-based technologies for biogas upgrading. Fuel 303, 121327. doi:10.1016/j.fuel.2021.121327.

Chilton, T.H., Colburn, A.P., 1934. Mass transfer (absorption) coefficients. Ind. Eng. Chem. Res. 26, 1183–1187.

Cuadri, A.A., Martín-Alfonso, J.E., Urbano, J., 2020. Using Mathcad to facilitate the design of chemical reactors involving multiple reactions. Comput. Appl. Eng. Educ. 28, 293–303. doi:10.1002/cae.22192.

Faramarzi, L., Kontogeorgis, G.M., Michelsen, M.L., Thomsen, K., Stenby, E.H., 2010. Absorber Model for CO2 Capture by Monoethanolamine, pp. 3751–3759. doi:10.1021/ie901671f.

Fuller, E.N., Schettler, P.D., Giddings, J.C., 1966. New method for prediction of binary gas-phase diffusion coefficients. Ind. Eng. Chem. 58, 18–27. doi:10.1021/ie50677a007.

Gabrielsen, J., Svendsen, H.F., Michelsen, M.L., Stenby, E.H., Kontogeorgis, G.M., 2007. Experimental validation of a rate-based model for CO2 capture using an AMP solution. Chem. Eng. Sci. 62, 2397–2413. doi:10.1016/j.ces.2007.01.034.

Garma, R., Binous, H., Dhaouadi, H., Bellagi, A., 2019. Design of continuous contacting countercurrent unit operations: an approach based on the usage of orthogonal collocation and <scp>Matlab</scp>. Comput. Appl. Eng. Educ. 27, 1308–1332. doi:10.1002/cae.22153.

Hartono, A., Mba, E.O., Svendsen, H.F., 2014. Physical properties of partially CO2 loaded aqueous monoethanolamine (MEA). J. Chem. Eng. Data 59, 1808–1816. doi:10.1021/je401081e.

Idris, Z., Han, J., Jayarathna, S., Eimer, D.A., 2017. Surface tension of alkanolamine solutions: an experimentally based review. Energy Procedia 114, 1828–1833. doi:10.1016/j.egypro.2017.03.1310.

Jakobsen, H.A., 2014. Chemical Reactor Modeling: Multiphase Reactive Flows, 2nd Ed. doi:10.1007/978-3-319-05092-8.

Jayarathna, S.A., Jayarathna, C.K., Kottage, D.A., Dayarathna, S., Eimer, D.A., Melaaen, M.C., 2013a. Density and surface tension measurements of partially carbonated aqueous monoethanolamine solutions. J. Chem. Eng. Data 58, 343–348. doi:10.1021/je300920t.

Jayarathna, S.A., Weerasooriya, A., Dayarathna, S., Eimer, D.A., Melaaen, M.C., 2013b. Densities and surface tensions of CO2 loaded aqueous monoethanolamine solutions with r = (0.2 to 0.7) at T = (303.15 to 333.15) K. J. Chem. Eng. Data 58, 986–992. doi:10.1021/je301279x.

Kim, I., Hoff, K.A., Hessen, E.T., Haug-Warberg, T., Svendsen, H.F., 2009. Enthalpy of absorption of CO2 with alkanolamine solutions predicted from reaction equilibrium constants. Chem. Eng. Sci. 64, 2027–2038. doi:10.1016/j.ces.2008.12.037.

Korson, L., Drost-Hansen, W., Millero, F.J., 1969. Viscosity of water at various temperatures. J. Phys. Chem. 73, 34–39. doi:10.1021/j100721a006.

Kvamsdal, H.M., Rochelle, G.T., 2008. Effects of the temperature bulge in CO2 absorption from flue gas by aqueous monoethanolamine. Ind. Eng. Chem. Res. 47, 867–875. doi:10.1021/ie061651s.

Lee, U., Burre, J., Caspari, A., Kleinekorte, J., Schweidtmann, A.M., Mitsos, A., 2016. Techno-economic optimization of a green-field post-combustion CO2 capture process using superstructure and rate-based models. Ind. Eng. Chem. Res. 55, 12014–12026. doi:10.1021/acs.iecr.6b01668.

Levenspiel, O., 1998. Chemical Reaction Engineering, 3rd ed. doi:10.1016/0009-2509(80)80132-1.

Luo, X., Hartono, A., Hussain, S., Svendsen, H.F., 2015. Mass transfer and kinetics of carbon dioxide absorption into loaded aqueous monoethanolamine solutions. Chem. Eng. Sci. 123, 57–69. doi:10.1016/j.ces.2014.10.013.

McCabe, W., Smith, J., Harriott, P., 2004. Unit Operations of Chemical Engineering, 7th Ed. McGraw-Hill.

Misic, D., Thodos, G., 1961. The thermal conductivity of hydrocarbon gases at normal pressures. AIChE J. 7, 264–267. doi:10.1002/aic.690070219.

Onda, K., Takeuchi, H., Okumoto, Y., 1968. Mass Transfer Coefficients Between Gas and Liquid Phases in Packed Columns. J. Chem. Eng. Japan 1, 56–62. doi:10.1252/jcej.1.56.

Peng, R., 1976. P-R.a New Equation of State. Proc. Natl. Acad. Sci. U. S. A. 15, 11–18.

Rocha, J.A., Bravo, J.L., Fair, J.R., 1993. Distillation columns containing structured packings: a comprehensive model for their performance. 1. Hydraulic Models. Ind. Eng. Chem. Res. 32, 641–651. doi:10.1021/ie00016a010.

Seader, J.D., Henley, E.J., 2004. Separation Process Principles, 2nd Ed. Wiley Series.

Snijder, E.D., Riele, M.J.M., Versteeg, G.F., 1993. Diffusion Coefficients of Several Aqueous Alkanolamine Solutions 475–480. https://doi.org/10.1021/je00011a037.

Stiel, L.I., Thodos, G., 1964. The thermal conductivity of nonpolar substances in the dense gaseous and liquid regions. AIChE J 10, 26–30. doi:10.1002/aic.690100114.

Suess, P., Spiegel, L., 1992. Hold-up of mellapak structured packings. Chem. Eng. Process. 31, 119–124. doi:10.1016/0255-2701(92)85005-M.

Taylor, R., Krishna, R., 1993. Multicomponent Mass Transfer. Wiley Series.

Tobiesen, F.A., Svendsen, H.F., Juliussen, O., 2007. Experimental Validation of a Rigorous Absorber Model for CO2 Postcombustion Capture 53. https://doi.org/10.1002/aic.

Tontiwachwuthikul, P., Meisen, A., Lim, C.J., 1992. CO2 absorption by NaOH, monoethanolamine and 2-amino-2-methyl-1-propanol solutions in a packed column. Chem. Eng. Sci. 47, 381–390. doi:10.1016/0009-2509(92)80028-B.

Vázquez, G., Alvarez, E., Navaza, J.M., Rendo, R., Romero, E., 1997. Surface tension of binary mixtures of water + monoethanolamine and water + 2-amino-2-methyl-1-propanol and tertiary mixtures of these amines with water from 25°C to 50°C. J. Chem. Eng. Data 42, 57–59. doi:10.1021/je960238w.

Wassiljewa, A., 1904. Warmeleitung in gasgemischen. Phys. Z.

Weiland, R.H., Dingman, J.C., Cronin, D.B., Browning, G.J., 1998. Density and viscosity of some partially carbonated aqueous alkanolamine solutions and their blends. J. Chem. Eng. Data 43, 378–382. doi:10.1021/je9702044.